ACS APPLIED MATERIALS & INTERFACES

Research Article

www.acsami.org

Fluorinated Benzothiadiazole (BT) Groups as a Powerful Unit for High-Performance Electron-Transporting Polymers

Junghoon Lee,[†,‡] Moonjeong Jang,[†,‡,§] Sang Myeon Lee,[‡] Dohyuk Yoo,[‡] Tae Joo Shin,[⊥] Joon Hak Oh,*[,§] and Changduk Yang*[,‡]

[‡]School of Energy and Chemical Engineering, KIER-UNIST Advanced Center for Energy, Low Dimensional Carbon Materials Center, Ulsan National Institute of Science and Technology (UNIST), Ulsan 689-798, South Korea

[§]Department of Chemical Engineering and [⊥]Pohang Accelerator Laboratory, Pohang University of Science and Technology (POSTECH), Pohang, Gyeongbuk 790-784, South Korea

Supporting Information

ABSTRACT: Over the past few years, one of the most remarkable advances in the field of polymer solar cells (PSCs) has been the development of fluorinated 2,1,3-benzothiadiazole (BT)-based polymers that lack the solid working principles of previous designs, but boost the power conversion efficiency. To assess a rich data set for the influence of the fluorinated BT units on the charge-transport characteristics in organic field-effect transistors (OFETs), we synthesized two new polymers (**PDPP-FBT** and **PDPP-2FBT**) incorporating diketopyrrolopyrrole (DPP) and either single- or double-fluorinated BT and thoroughly investigated them via a range of techniques. Unlike the small differences in the absorption properties of **PDPP-FBT** and its nonfluorinated analogue (**PDPP-BT**), the introduction of doubly fluorinated BT into the polymer backbone induces a noticeable change in its optical profiles and energy levels, which results in a slightly wider bandgap and deeper HOMO for **PDPP-2FBT**, relative to the others. Grazing incidence X-ray diffraction (GIXD) analysis reveals that both fluorinated polymer films have long-range orders along the out-of-plane direction, and $\pi-\pi$ stacking in the in-plane direction, implying semicrystalline lamellar structures with edge-on orientations in the solid state. Thanks to the strong intermolecular interactions and highly electron-deficient π-systems driven by the inclusion of F atoms, the polymers exhibit electron mobilities of up to 0.42 and 0.30 $cm^2\ V^{-1}\ s^{-1}$ for **PDPP-FBT** and **PDPP-2FBT**, respectively, while maintaining hole mobilities higher than 0.1 $cm^2\ V^{-1}\ s^{-1}$. Our results highlight that the use of fluorinated BT blocks in the polymers is a promising molecular design strategy for improving electron transporting performance without sacrificing their original hole mobility values.

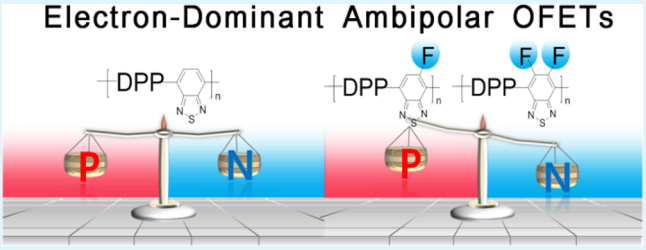

KEYWORDS: *n-channel dominant FET, fluorinated benzothiadiazole, diketopyrrolopyrrole, fluorine, organic field-effect transistors (OFET)*

INTRODUCTION

The use of solution-processable semiconducting polymers for organic field-effect transistors (OFETs) continues to attract considerable interest, because polymeric systems can offer the possibility of cheap raw materials, low processing costs, excellent film formation, and mechanical properties such as flexibility and large-area uniformity.[1−12] Recently, diketopyrrolopyrrole (DPP)-based donor−acceptor (D−A) polymers have been widely developed, and have proven themselves to be one of the most promising semiconductors for high-performance unipolar *p*-channels and *p*-channel-dominant ambipolar OFETs (with hole mobilities exceeding 3 $cm^2\ V^{-1}\ s^{-1}$).[13−18] Nonetheless, the development of DPP-based polymers with high-performance *n*-channel charge transport has lagged behind that of the aforementioned *p*-channel dominant polymers, primarily due to the inherent instability of the electron charge carriers in the presence of ambient oxidants such as O_2, H_2O, or O_3.[9]

The research efforts of our groups have recently focused on developing high electron-affinity polymers based on DPP, using a structural modification of the conventionally used 2,1,3-benzothiadiazole (BT) acceptor moiety. For example, by copolymerizing with a stronger acceptor bis-benzothiadiazole (BBT) unit relative to BT, the resulting polymer (PDPP-BBT) showed even *n*-channel dominant characteristics, yet yielded unsatisfactory electron mobility results ($\sim 1 \times 10^{-3}$ $cm^2\ V^{-1}\ s^{-1}$).[19] In the meantime, many other groups have often highlighted the use of fluorinated BT units into the polymer backbone, and demonstrated improved photovoltaic performance.[20−27] Although the cause of the efficiency improvement varies noticeably depending upon the specific systems, it is generally recognized that the inclusion of fluorine (F) atoms

Received: September 1, 2014
Accepted: October 13, 2014
Published: October 13, 2014

Scheme 1. Synthetic Routes to PDPP-FBT and PDPP-2FBT[a]

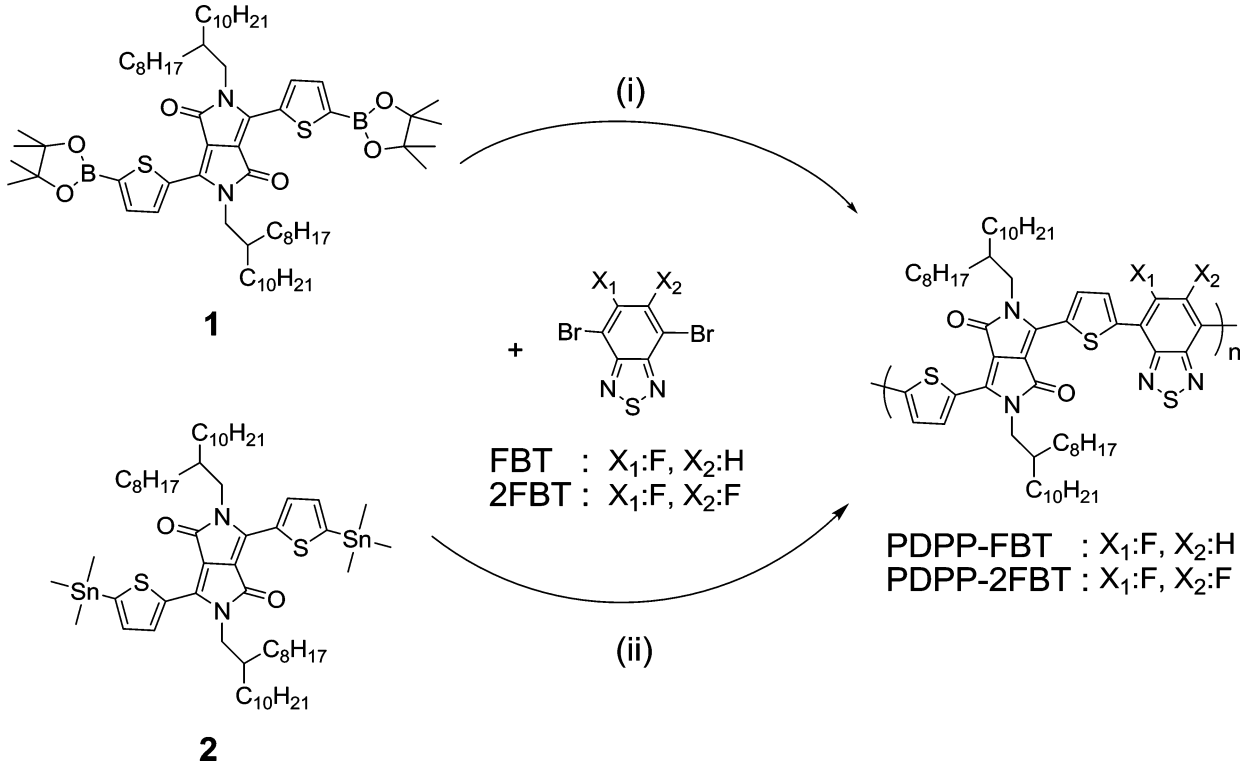

[a]Suzuki polycondensation conditions (i): $Pd_2(dba)_3$, P(*o*-tolyl)$_3$, K_3PO_4, toluene/H_2O, 95 °C; Stille polycondensation conditions (ii): $Pd_2(dba)_3$, P(*o*-tolyl)$_3$, toluene, 120 °C, microwave.

can not only fine-tune the energy levels of polymers, but also promote noncovalent interactions through C−F···H, F···S on mesoscopic solid-state structures.[26−28] In addition, it is well-known that the strong electron-withdrawing nature of F atoms allows for efficient electron injection into the LUMO and increases hydrophobicity, which can increase the electron affinity and environmental stability of semiconductors in OFET operations, relative to their fluorine-free analogues.[29−34]

These early results motivated us to design DPP-based polymers containing the ubiquitous fluorinated BT blocks (FBT (1F) and 2FBT (2F)), with a view to assessing semiconductors with high electron mobility and high environmental stability. Herein, as an attempt to investigate the effects of fluorinated BT blocks on the charge-carrier transport properties in OFETs, we report on the synthesis and characterization of poly(3,6-dithien-2-yl-2,5-di(2-octyldodecyl)-pyrrolo[3,4-*c*]pyrrole-1,4-dione-5′,5″-diyl-*alt*-fluorobenzo 2,1,3-thiadiazol-4,7-diyl] and poly(3,6-dithien-2-yl-2,5-di(2-octyldodecyl)-pyrrolo[3,4-*c*]pyrrole-1,4-dione-5′,5″-diyl-*alt*-difluorobenzo 2,1,3-thiadiazol-4,7-diyl] (**PDPP-FBT** and **PDPP-2FBT**, see Scheme 1), and show the differences in their optophysical and redox properties, molecular packings, and OFET performances. Furthermore, we elucidate how the degree of the substitution of F atoms on a BT unit affects the charge-carrier mobilities and the dynamics of dominant polarity by comparison with a nonfluorinated analogue (**PDPP-BT**), and finally discuss the overall structure-property relationship.

RESULT AND DISCUSSION

Synthetic Strategies, Synthesis, and Characterization. The fluorinated BT (FBT and 2FBT) and diboronic ester DPP derivatives were easily synthesized according to the established methods.[26,35] Polymerization of the FBT and 2FBT monomers using standard palladium(0)-catalyzed Suzuki polycondensation with the diboronic ester comonomer produced the corresponding polymers (**PDPP-FBT** and **PDPP-2FBT**). However, the number-average molecular weight (M_n) was below 10 kDa with a polydispersity index (PDI) of approximately 2.5 for both the polymers, as determined by gel permeation chromatography (GPC) in THF after Soxhlet purification. It has been reported that a high molecular weight can play an important role in achieving nanometer-sized interconnected morphologies, hence resulting in efficient channels for charge-carrier transport via a hopping mechanism.[11,36] Thereby, the observed relatively low molecular weights prompted us to screen various Suzuki coupling conditions, such as the utilization of a microwave-assisted heating protocol, the use of tiny amounts of catalyst, varying the solution concentration, the replacement of $Pd(PPh_3)_4$ with $Pd_2(dba)_3$ as a catalyst, and different ligand/palladium ratios, in order to improve the molecular weights. Nevertheless, the attempted synthesis of the polymers by Suzuki polymerization only afforded undesired low molecular weight materials, possibly due to either the competing base- and/or metal-catalyzed protodeborylation of the electron-rich thiophenes adjacent to the DPP monomer under our reaction conditions.[37−40] In addition, we found no appreciable difference in the molecular weight, even if the monomer was diiodo BT. Therefore, we decided to apply a Stille polycondensation instead of the Suzuki one, because the Stille-coupling reaction is generally recognized as a better alternative to the Suzuki protocol, when electron-rich species (thiophenes or pyrroles) are coupled.[41,42] Thus, the key DPP monomer, distannyl DPP was prepared by lithiation using diisopropylamide (LDA) and

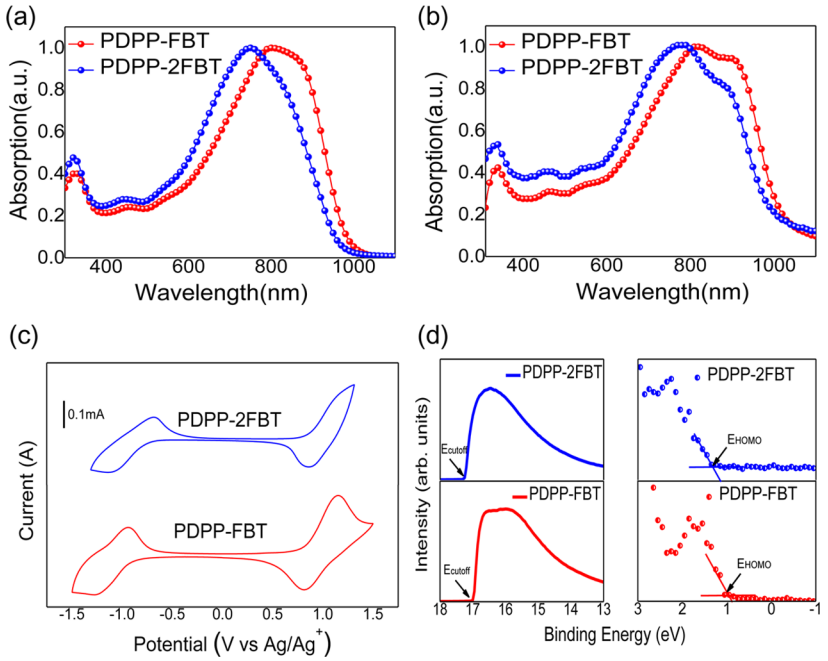

Figure 1. UV−vis−NIR absorption spectra of **PDPP-FBT** and **PDPP-2FBT** in dilute chloroform (a) solution and (b) thin film on glass plate. (c) Cyclic voltammograms of **PDPP-FBT** and **PDPP-2FBT**. (d) UPS spectra of **PDPP-FBT** and **PDPP-2FBT**.

subsequent quenching with trimethyltin chloride. Stille polymerization under microwave heating conditions was employed to form the **PDPP-FBT** and **PDPP-2FBT** respectively, which indeed proceeded in good yields (75−80%), with sufficiently high molecular weights (M_n of 24.0 kDa and 25.0 kDa with PDIs of 2.01 and 2.34 for **PDPP-FBT** and **PDPP-2FBT**, respectively, as determined by GPC and THF eluent). Both polymers were soluble in common organic solvents such as tetrahydrofuran, chloroform, toluene, and chlorobenzene.

The UV−vis−NIR absorption spectra of the polymers in chloroform solution and in a solid state are shown in panels a and b in Figure 1. The absorption data are listed in Table 1.

Table 1. Optical and Electrochemical Properties of PDPP-FBT and PDPP-2FBT

	UV			CV			UPS
polymer	λ_{max}^{sol} (nm)[a]	λ_{max}^{film} (nm)[b]	E_g^{opt} (eV)[c]	E_{HOMO} (eV)[d]	E_{LUMO} (eV)[d]	E_g^{CV} (eV)[e]	E_{IP}^{UPS} (eV)[f]
PDPP-FBT	798	816	1.20	−5.22	−3.49	1.73	5.38
PDPP-2FBT	750	772	1.26	−5.37	−3.53	1.84	5.48

[a]Chloroform solution. [b]Spin-coated from chloroform solution. [c]Determined from the onset of the electronic absorption spectra. [d]Cyclic voltammetry determined with (E_{HOMO} = -($E_{(OX)}^{onset}$ + 4.4 eV) and (E_{LUMO} = -($E_{(Red)}^{onset}$ + 4.4 eV); [e]$E_g^{CV} = E_{LUMO} - E_{HOMO}$; [f]$E_{IP}^{UPS} = h\nu - (E_{cutoff} - E_{HOMO})$, incident photon energy ($h\nu$ = 21.2 eV) for He I.

Upon changing from solutions to films, the absorption peaks for both polymers are not only red-shifted (~20 nm) and broadened to some extent, but also their low-energy shoulder bands at the range of 870−910 nm are intensified, presumably because of the occurrence of the aggregation or $\pi-\pi$ stacking in solid state. This is a common phenomenon for rigid conjugated polymers.[43,44] Very interestingly, although the spectral profile of **PDPP-FBT** is nearly identical to that of the nonfluorinated **PDPP-BT** (See Figure S1 in Supporting Information),[43,45] the increment in the number of F atoms from 1 to 2 on the repeating unit leads to a blue shift in the absorption onset (λ_{onset}) and maximum (λ_{max}) of the polymer. This results in a larger optical band gap of **PDPP-2FBT** (E_g^{opt} = 1.26 eV), which is 0.06 eV larger than that of **PDPP-FBT** (E_g^{opt} = 1.20 eV). Therefore, one can conclude that the inclusion of one F atom on the BT unit of **PDPP-BT** hardly affects the absorption characteristics, but the incorporation of two F atoms can alter the intrinsic optical properties, compared to the nonfluorinated **PDPP-BT**.

Cyclic voltammetry (CV) reveals reversible oxidation/reduction behaviors for both polymers, with the **PDPP-2FBT** being oxidized at a voltage that is 0.15 eV higher, relative to the **PDPP-FBT** (Figure 1c). In addition, the ionization potential (IP) values of each polymer measured by ultraviolet photoelectron spectroscopy (UPS) (Figure 1d and Table 1) show similar trends with slight differences in their energy levels. On the other hand, the LUMO of **PDPP-2FBT** is −3.53 eV, which is 0.04 eV lower than that of **PDPP-FBT** (−3.49 eV), implying that doubly fluorinated BT effectively lowers the HOMO level with only a minor effect on the LUMO.

The computational calculations were carried out on the trimer systems of each polymer using density functional theory (DFT) with the B3LYP hybrid functional and the 6-311G(d) basis set, as implemented in Gaussian 09. Figure 2 presents the adopted planar conformation with extremely small torsional angles for both cases, showing excellent coplanarity. In addition, both the HOMO and LUMO isosurfaces for the two model oligomers show delocalized characteristics, indicating the high possibility of ambipolar charge transport. Notably, upon taking a closer look at these structures, their HOMO isosurfaces were relatively more localized on the lateral axis π-systems, when compared to that observed for the nonfluorinated **PDPP-BT** (see Figure S2 in the Supporting Information). Thereby, both fluorinated polymers would

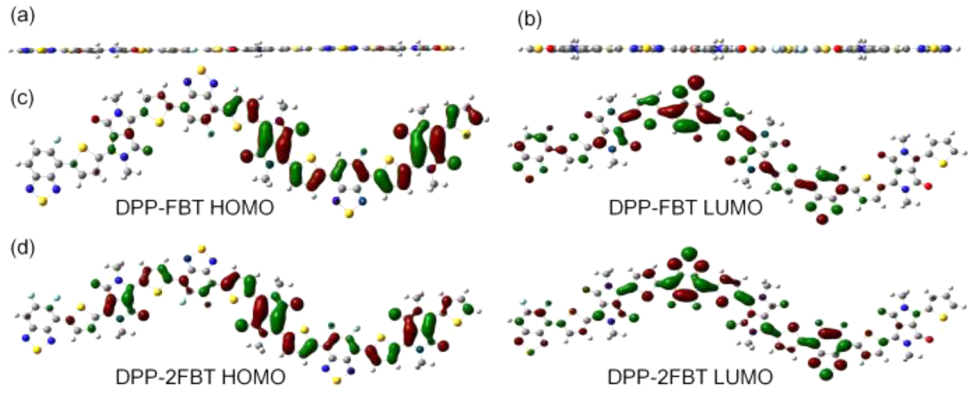

Figure 2. Calculated side view of model trimers for (a) DPP-FBT and (b) DPP-2FBT; DFT-optimized geometries and charge-density isosurfaces for (c) DPP-FBT and (d) DPP-2FBT HOMO and LUMO levels.

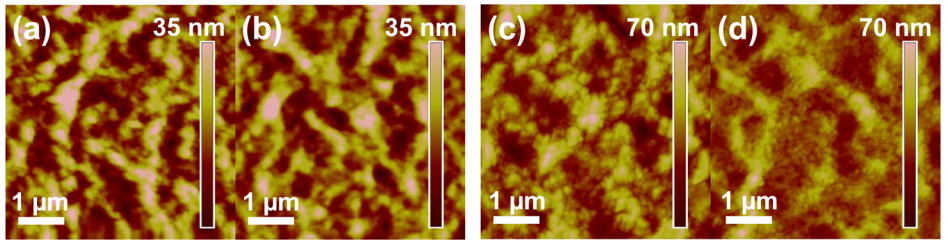

Figure 3. AFM height images (5 μm × 5 μm) of drop-cast (a, b) **PDPP-FBT** and (c, d) **PDPP-2FBT** films (a, c) before and (b, d) after the thermal annealing at 250 °C, on OTS-modified SiO_2/Si substrates. RMS roughness: (a) = 7.67 nm, (b) = 6.90 nm, (c) = 11.80 nm, (d) = 8.57 nm.

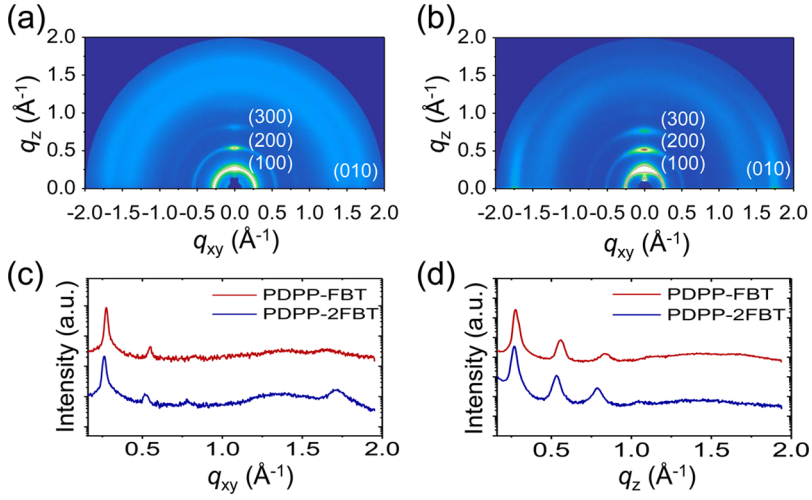

Figure 4. 2D-GIXD images of drop-cast films of fluorinated DPP-BT polymers annealed at 250 °C: (a) **PDPP-FBT** and (b) **PDPP-2FBT**. The corresponding GIXD diffractogram profiles: (c) in-plane and (d) out-of-plane GIXD patterns.

strengthen their electron charge-carrier transport and be expected to afford *n*-channel dominant ambipolar OFETs, in line with our aforementioned hypothesis. After the optimization of the geometrical structures, time-dependent DFT (TD-DFT) calculations for the polymer repeating unit were also performed for the analysis of the backbone chain dipole dependence (see Table S1 in the Supporting Information). The single unit of **PDPP-FBT** shows a larger change in dipole on transition from the ground to excited states ($\Delta\mu_{ge}$) than that of **PDPP-2FBT**, most likely due to the asymmetry-induced odd-numbered F-substitute on BT motif (see Figure S3 and Table S1 in the Supporting Information). Even though the current level of the theory above can only provide general trends, this database would be a useful benchmark for predicting the effect of more subtle structural modifications with fluorination for conjugated polymers.

Thin-Film Microstructure Analysis. The film morphologies of fluorine-substituted conjugated polymers were examined using tapping-mode atomic force microscopy (AFM). The polymer films were drop-casted onto *n*-octadecyltrimethoxysilane (OTS)-modified SiO_2/Si substrate from the polymer solution (~5 mg mL^{-1}) using 1,2,4-trichlorobenzene (bp = 214 °C) as the solvent. The drop-casting method typically provides a longer drying time than a spin-coating technique and enables the formation of films with a higher degree of crystallinity. The use of solvents with high-boiling points is known to be beneficial for forming higher crystallinity structures and larger crystal sizes, typically leading to enhanced performance in

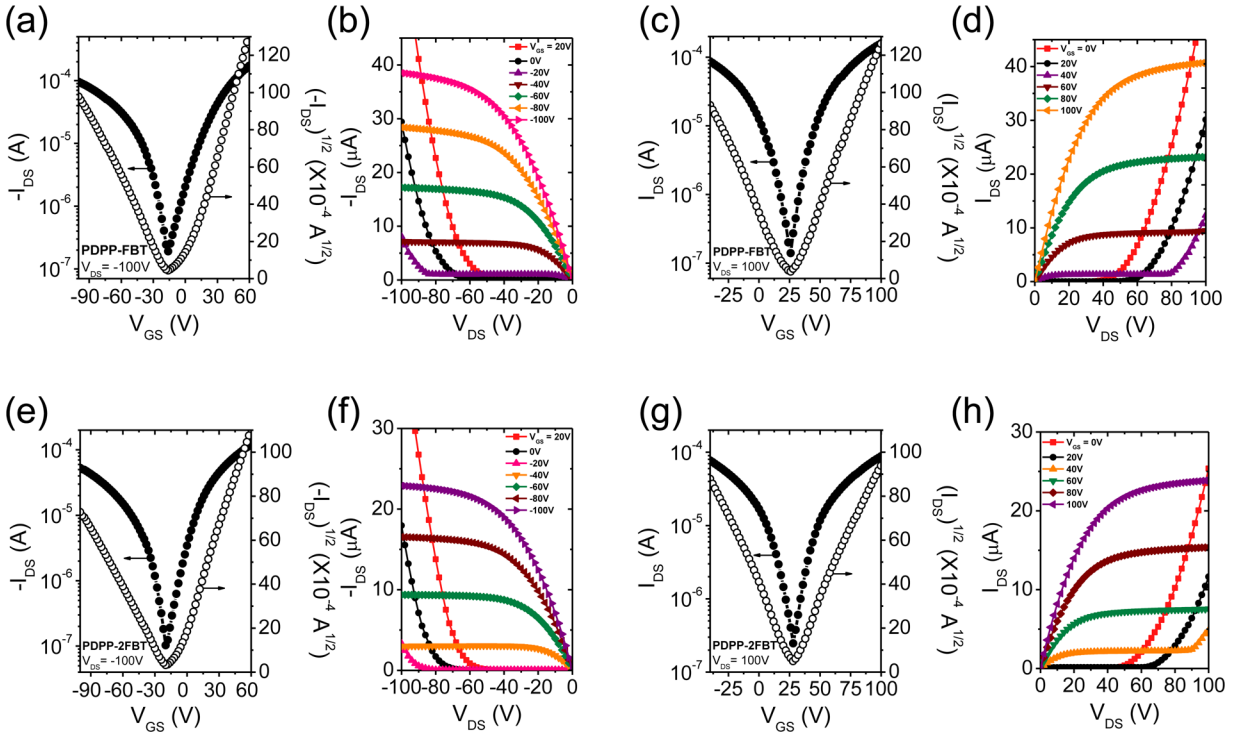

Figure 5. Current−voltage (*IV*) characteristics of OFETs based on ambipolar (a–d) **PDPP-FBT** and (e–h) **PDPP-2FBT** films of annealed at 250 °C. Transfer characteristics for polymer films in (a, e) *p*-channel operation (V_{DS} = −100 V) and (c, g) *n*-channel operation (V_{DS} = +100 V) mode. (b, d, f, and h) Output characteristics for **PDPP-FBT** and **PDPP-2FBT** films.

Table 2. Summary of OFETs Performance Data Based on PDPP-FBT and PDPP-2FBT Films

sample[a]		*p*-channel				*n*-channel			
polymer	condition	$\mu_{h,max}$[c] ($cm^2 V^{-1} s^{-1}$)	$\mu_{h,avg}$[d] ($cm^2 V^{-1} s^{-1}$)	I_{on}/I_{off}	V_T (V)	$\mu_{e,max}$ ($cm^2 V^{-1} s^{-1}$)	$\mu_{e,avg}$ ($cm^2 V^{-1} s^{-1}$)	I_{on}/I_{off}	V_T (V)
PDPP-FBT	without annealing	0.087	0.060 (±0.020)[e]	>1 × 10^4	−6.4	0.061	0.044 (±0.013)	>1 × 10	36.6
	thermal annealing[b]	0.21	0.15 (±0.03)	>1 × 10^2	−17.5	0.42	0.33 (±0.05)	>1 × 10^3	30.9
PDPP-2FBT	without annealing	0.033	0.023 (±0.004)	>1 × 10^4	−7.1	0.029	0.016 (±0.001)	>1 × 10^2	32.8
	thermal annealing	0.10	0.077 (±0.021)	>1 × 10^2	−19.1	0.30	0.19 (±0.07)	>1 × 10^2	28.6

[a]The *p*-channel and *n*-channel characteristics of ambipolar OFETs were measured in a nitrogen atmosphere. [b]Thermal annealing was applied at 250 °C. [c]The maximum mobility of the OFET devices (L = 50 μm and W = 1000 μm). [d]The average mobility of the OFET devices (L = 50 μm and W = 1000 μm). [e]The standard deviation was carried out by using more than 10 devices.

OFETs.[46−49] The drop-cast **PDPP-FBT** and **PDPP-2FBT** films exhibited granular structures (Figure 3). Remarkably, the as-cast polymer films showed relatively larger void areas and more distinct grain boundaries between crystalline domains, whereas the polymer films that were annealed at 250 °C for 30 min exhibited interconnected granular domains with more smooth surfaces. The **PDPP-2FBT** film had smaller granular domains with a larger root-mean-square (RMS) roughness value of 8.6 nm, compared with that (6.9 nm) of the **PDPP-FBT** film. In addition, the optimized drying time for the preparation of **PDPP-FBT** films was significantly longer (about 1.5 times) than that of the **PDPP-2FBT** films. A longer drying time typically leads to the formation of polymer films with enhanced crystallinity.[47−49]

Two-dimensional grazing incidence X-ray diffraction (2D GIXD) analyses of the drop-cast films were also performed to investigate the effects of the F-containing benzothiadiazole moieties of the DPP-based polymers on the crystallinity and molecular packing further. Figure 4 shows 2D GIXD images and the corresponding diffractogram profiles of the annealed **PDPP-FBT** and **PDPP-2FBT** films. The calculated crystallographic parameters are summarized in Table S2 in the Supporting Information. **PDPP-FBT** and **PDPP-2FBT** both exhibited well-defined diffraction peaks up to (300) diffraction in the out-of-plane directions, indicating that fluorinated polymers have a long-range ordered lamellar packing. Both polymer films displayed strong (100) diffractions at q_z values of 0.28 and 0.27 $Å^{-1}$, corresponding to *d*-spacings of 22.8 and 23.4 Å, respectively. It is known that fluorine−sulfur interactions can facilitate the planarization of the polymer backbone, leading to a reduction in the intermolecular packing distances.[24,46,50] However, the *d*(100)-spacing of the **PDPP-2FBT** film was larger than that of the **PDPP-FBT** film. This is presumably due to the increase in the number of bulky F atoms and the electrostatic repulsion between F atoms.[51] **PDPP-FBT** and **PDPP-2FBT** showed discernible (010) diffraction peaks in the in-plane direction, which corresponded to π−π stacking (π-stack distance ∼3.8 Å). These results indicate that both polymers have a strong preference for edge-on molecular orientations that are effective for charge transport between

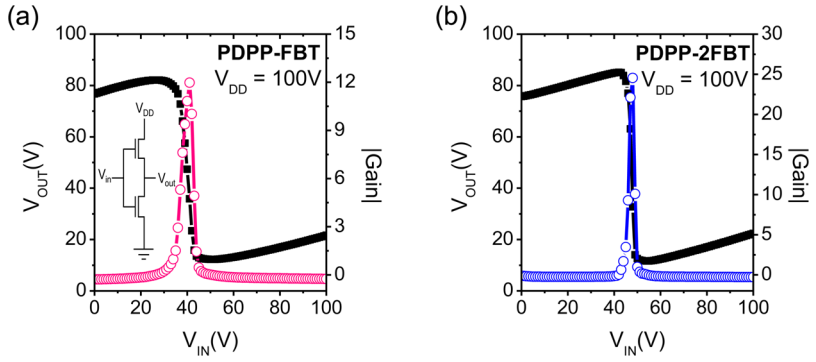

Figure 6. Inverter characteristic based on (a) ambipolar **PDPP-FBT** and (b) **PDPP-2FBT** OFETs (V_{DD} = 100 V).

source and drain electrodes.[52] The annealed polymer films exhibited decreased $d(100)$-spacings and increased coherence lengths, when compared to those of the as-cast films (see Figure S4 in the Supporting Information for the 2D GIXD images and the corresponding diffractogram profiles of the as-cast films). This indicates that the polymer films exhibit denser molecular packing after the thermal annealing.

OFET Performance. To investigate the electrical performance of F-substituted DPP-BT polymers, top-contact bottom-gate OFET devices were constructed with **PDPP-FBT** and **PDPP-2FBT** films as the semiconducting layer. The details about OFET fabrication are included in the Experimental Section. Figure 5 exhibits the typical V-shaped ambipolar characteristics of OFETs based on **PDPP-FBT** and **PDPP-2FBT** films after thermal annealing. $I-V$ characteristics of the as-prepared films are also presented in Figure S6 in the Supporting Information. The electrical performance characteristics such as charge carrier mobilities, on/off ratios, and threshold voltages are listed in Table 2. The electrical performance of the F-substituted DPP-BT polymers was enhanced after thermal annealing. This is mainly due to the denser molecular packing characteristic after thermal annealing, as described in the Thin-Film Microstructure Analysis section. The enhancement in electron mobility was relatively larger than that of the hole mobility after the thermal annealing. It has been reported that the trap density of electrons by ambient oxidants commonly tends to decrease after proper thermal annealing, leading to enhanced electron mobility in ambipolar semiconductors.[5,53] As a control experiment, we also tested the electrical performance of **PDPP-BT** OFETs with gold contacts. The thermally annealed **PDPP-BT** OFETs exhibited hole-dominant ambipolar transport behaviors, with the optimized hole and electron mobilities of up to 0.11 and 0.076 $cm^2\ V^{-1}\ s^{-1}$, respectively (see Table S3 in the Supporting Information). In general, the injection barriers of electrons from the gold electrode (work function ~5.1 eV) to the LUMO were usually much larger than to the HOMO, because of the high-lying LUMO of the common polymer semiconductors, and the current flow is typically dominated by hole transport. In our experiment, the introduction of fluorine atoms into the main backbone of the BT unit effectively lowered the energy levels of the resulting polymers. The respective HOMO levels of the **PDPP-BT**, **PDPP-FBT**, and **PDPP-2FBT** are −5.10, −5.38, and −5.48 eV, whereas their respective LUMO levels are −3.90, −4.18, and −4.22 eV, because of the increase in the number of electron-withdrawing fluorine substituents. Consequently, the hole injection barriers from gold to F-substituted polymers would increase, while the electron injection barriers would decrease. Therefore, both F-substituted polymers exhibited electron-dominant ambipolar transport behavior after optimization (Table 2). However, the **PDPP-FBT** films showed a better electrical performance than **PDPP-2FBT** films, despite their higher LUMO and HOMO energy levels that are less favorable for the electron charge-carrier transport. The OFETs based on annealed **PDPP-FBT** films exhibited the maximum electron and hole mobilities of 0.42 and 0.21 $cm^2\ V^{-1}\ s^{-1}$, whereas the average electron and hole mobilities were 0.33 ± 0.05 and 0.15 ± 0.03 $cm^2\ V^{-1}\ s^{-1}$, respectively. On the other hand, the OFETs constructed with the annealed **PDPP-2FBT** films showed the maximum electron and hole mobilities of 0.30 and 0.10 $cm^2\ V^{-1}\ s^{-1}$, with the average electron and hole mobilities of 0.19 ± 0.07 and 0.077 ± 0.021 $cm^2\ V^{-1}\ s^{-1}$, respectively. These results can be attributed to the morphological factors, rather than to the energy levels. As shown by AFM and GIXD results, the **PDPP-FBT** films exhibited denser molecular packing with much larger grains. These findings indicate that the charge transport in these fluorinated polymers is significantly affected by the morphological features, in addition to energetic factors.

Two ambipolar transistors based on fluorinated DPP-BT polymers were integrated into the complementary metal-oxide-semiconductor (CMOS)-like inverters. Figure 6 shows the output voltage (V_{OUT}) as a function of the input voltage (V_{IN}) at a constant supply voltage (V_{DD}) of 100 V. The gate voltage is the circuit input voltage, which varies from 0 V to V_{DD}. At a small input voltage (V_{IN}), the *p*-channel transistor was on, and the *n*-channel transistor was off. The inverter of **PDPP-FBT** with high charge carrier mobilities of both holes and electrons exhibited a gain of 12. However, a higher gain value of 25 was recorded from the **PDPP-2FBT** inverters. Furthermore, the sharp switching of the circuits was shifted to nearly $V_{DD}/2$ in **PDPP-2FBT**. This result is most likely due to the higher symmetry of the threshold voltages of **PDPP-2FBT** transistors in *p*- and *n*-channel operation modes.[6,54,55]

CONCLUSION

Two conceptually identical polymers apart from having a different number of F atoms on their repeating unit (**PDPP-FBT** (one F) and **PDPP-2FBT** (two F)) were synthesized and carefully investigated in a comparative manner, in order to understand the effects of introducing fluorinated BT moieties into DPP polymers. Although **PDPP-FBT** shows very similar optical properties to those of its nonfluorinated analogue (**PDPP-BT**); interestingly, a noticeable change in the optical profiles and energy levels is observed by increasing the number of F atoms on the BT unit atom from 1 to 2, thereby resulting

in a wider bandgap and deeper HOMO for **PDPP-2FBT**, relative to the others. In GIXD analysis, the films of both polymers appear to have strong lamellar textures with three out-of-plane peaks and a $\pi-\pi$ stacking peak in the in-plane diffraction, indicating that the polymers adopt a preferential edge-on orientation relative to the substrates. To our delight, the fluorinated polymers FETs exhibited high electron mobilities of up to 0.42 $cm^2\ V^{-1}\ s^{-1}$, together with hole mobilities as high as 0.21 $cm^2\ V^{-1}\ s^{-1}$. These results are rationalized through a combination of the stronger intermolecular noncovalent interactions and higher electron-affinity π-systems, both of which can be induced from the F substituents. Not only does this study therefore provide new insights into charge-transport characteristics and our understanding of semiconducting polymers with incorporated fluorinated BT units, but also offers a powerful strategy for the molecular design of high-performance *n*-channel OFETs.

EXPERIMENTAL SECTION

General Procedures and Methods. All starting materials were purchased either from Aldrich or Acros and used without further purification. All solvents are ACS grade unless otherwise noted. Anhydrous THF was obtained by distillation from sodium/benzophenone prior to use. Anhydrous toluene was used as received. 3,6-Bis(5-(4,4,5,5-tetramethyl-1,3,2-dioxaborolan-thiophene-2-yl)-2,5-bis(2-octyldodecyl)-pyrrolo[3,4-*c*]pyrrole-1,4-dione (DPP) was prepared according to established literature procedures.[35] ^{1}H NMR and ^{13}C NMR spectra were recorded on a VNMRS 600 (Varian, USA) spectrophotometer and 400-MR DD2 (Agilent) using $CDCl_3$ and $C_2D_2Cl_4$ as solvent and tetramethylsilane (TMS) as the internal standard and MALDI MS spectra were obtained from Ultraflex III (Bruker, Germany). UV−vis−NIR spectra were taken on Cary 5000 (Varian USA) spectrophotometer. Microwave reactions were performed by Microwave Synthesis Reactor (Microwave, Anton Paar). DFT calculations were performed using the Gaussian 09 package with the nonlocal hybrid Becke three-parameter Lee−Yang−Parr (B3LYP) function and the 6-311G basis set to elucidate the HOMO and LUMO levels after optimizing the geometry of DPP-BT, DPP-FBT, and DPP-2FBT trimer using the same method and time-dependent self-consistent field (TD-SCF) approximation was used for excited state dipole moment. Number-average (M_n) and weight-average (M_w) molecular weights, and polydispersity index (PDI) of the polymer products were determined by gel permeation chromatography (GPC) with Waters 150C GPC using a series of mono disperse polystyrene as standards in THF (HPLC grade). Cyclic voltammetry (CV) measurements were performed on Solartron electrochemical station (METEK, Versa STAT3) with a three-electrode cell in a 0.1 M tetra-*n*-butylammonium hexafluorophosphate (*n*-Bu_4NPF_6) solution in acetonitrile at a scan rate of 100 mV/s at room temperature under argon. Ag/Ag^+ electrode, a platinum wire and a glass carbon disk were used as the reference electrode, counter electrode, and working electrode, respectively. The HOMO energy levels were obtained from the equation HOMO (eV) = $-(E_{(ox)}{}^{onset} + 4.4)$. The LUMO levels of polymers were obtained from the equation LUMO (eV) = $-(E_{(red)}{}^{onset} + 4.4)$. Ultraviolet photoelectron spectroscopy (UPS) was examined by AXIS-NOVA CJ109, Kratos. The polymer solution was prepared in chloroform with 5 mg mL^{-1} for **PDPP-BT**, **PDPP-FBT**, and **PDPP-2FBT**. The **PDPP-BT**, **PDPP-FBT**, and **PDPP-2FBT** solution was spin-coated on indium tin oxide (ITO) glass films, respectively. Film fabrication was done in a N_2-atmosphere glovebox. The UPS analysis chamber was equipped with a hemispherical electron-energy analyzer (Kratos Ultra Spectrometer), and was maintained at 1.0×10^{-9} Torr. The UPS measurements were carried out using the He I ($h\nu$ = 21.2 eV) source. Thermogravimetric analysis (TGA) was performed by Simutaneous DSC/TGA instrument (TA Instruments, USA) at the heating rate of 10 °C min^{-1}. Differential scanning calorimetry (DSC) curves were recorded by differential scanning calorimeter (TA Instruments, USA) at the heating rate of 10 °C min^{-1}.

OFET Device Fabrication and Characterization. OFETs were fabricated in the top-contact bottom-gate configuration using a SiO_2/Si wafer. A 300 nm-thick SiO_2 layer (capacitance per unit area, C_i = 10 nF cm^{-2}) and the underlying highly *n*-doped Si (<0.004 Ω·cm) were utilized as the gate dielectric and the gate electrode, respectively. The SiO_2 surface was modified with *n*-octadecyltrimethoxysilane (OTS) based self-assembled monolayer (SAM). Prior to the treatment of OTS SAM, the SiO_2 surface contamination was removed using Piranha (H_2SO_4 + H_2O_2) solution. The SiO_2/Si substrates were washed sequentially with deionized water and then used the UV-ozone treatment. The OTS solution (3 mM in trichloroethylene) was spin-coated on the cleaned substrate at 3000 rpm then, the substrates placed in a vacuum desiccator with NH_4OH vapor for overnight. The OTS solution treatment was used to remove OH groups from the SiO_2 surface, and to optimize dielectric/semiconductor interface. The SiO_2/Si substrates were washed with toluene, acetone, and isopropyl alcohol and dried by blowing nitrogen gas. The polymeric semiconducting layer was deposited on the cleaned substrates by drop casting. The polymer solution (~5 mg mL^{-1}) was prepared in 1,2,4-trichlorobenzene and filtered through a 0.22 μm syringe filter. The films were dried in vacuum oven at 100 °C to remove solvent residue. Then the **PDPP-FBT** and **PDPP-2FBT** thin films were annealed at 250 °C for 30 min on a hot plate. All the samples were fabricated inside a nitrogen-filled glovebox. A 40 nm thick gold layer was thermally deposited through a shadow mask to form the source and drain electrodes. OFETs have a channel length (L) of 50 μm and a channel width (W) of 1000 μm with W/L = 1000 μm/50 μm = 20. The transfer and output characteristics of ambipolar **PDPP-FBT** and **PDPP-2FBT** OFETs were measured by using a Keithley 4200 semiconductor parametric analyzer under nitrogen atmosphere. The carrier mobility was calculated in the saturated regime according to the equation:

$$I_{DS} = (W/2L)\mu C_i(V_G - V_T)^2$$

where I_{DS} is the drain current, W and L are the semiconductor channel width and length, respectively, μ is the mobility, C_i is the capacitance per unit area of the gate dielectric layer, and V_G and V_T are, respectively, the gate voltage and threshold voltage.

2,5-Bis(2-octhyldodecyl)-3,6-bis(5-(trimethylstannyl)thiophen-2-yl) pyrrolo[3,4-*c*]pyrrole-1,4-dione (2). Compound **2** was prepared according to established literature procedures.[56] Isolated yield = 420 mg (87%). ^{1}H NMR (400 MHz, $CDCl_3$, δ): 8.99 (d, J = 3.66 Hz, 2H), 7.32 (d, J = 3.66 Hz, 2H), 4.05 (d, J = 7.66 Hz, 4H), 1.97−1.92 (m, 2H), 1.21−1.30 (m, 64H), 0.83−0.88 (m, 12H), 0.43 (s, 18H); ^{13}C NMR (100 MHz, $CDCl_3$, δ): 161.77, 145.68, 139.79, 136.10, 135.94, 135.32, 107.22, 46.14, 37.89, 31.91, 31.39, 30.06, 29.64, 29.62, 29.59, 29.53, 29.34, 29.29, 26.40, 22.68, 22.65, 14.11, −8.10. Anal. Calcd for $C_{60}H_{104}N_2O_2S_2Sn_2$: C 60.71, H 8.83 N, 2.36, S, 5.40. Found: C 61.04, H 9.53, N 2.69.

Typical Procedure for Suzuki coupling Polymerization and Polymer Purification. Boronic ester DPP (0.20 mmol), dibromo FBT or 2FBT (0.20 mmol), tris(dibenzylidenacetone) dipalladium (0) (1.7 mg, 2.0 μmmol), anhydrous toluene (4 mL) were mixed in a Schlenk flask which was purged with argon for 30 min. To this solution, tri(*o*-tolyl)phosphine (1.2 mg, 4.0 μmol) and K_3PO_4 in demineralized water (2 mL) were added and the reaction mixture was heated at 95 °C under vigorous stirring for 48 h. The crude product was poured into a mixture of methanol (300 mL). The resulting solid was filtered off and subjected to sequential Soxhlet extraction with methanol (1 d), acetone (1 d) to remove the low molecular weight fraction of the materials. The residue was extracted with chloroform in order to produce a dark purple product after precipitating again from methanol and drying in vacuo.

Poly(3,6-dithien-2-yl-2,5-di(2-octyldodecyl)-pyrrolo[3,4-*c*]-pyrrole-1,4-dione-5′,5″-diyl-*alt*-fluorobenzo 2,1,3-thiadiazol-4,7-diyl] (PDPP-FBT). Isolated yield of polymer PDPP-FBT = 100 mg (50%). GPC analysis M_n = 6.1 kg/mol, M_w = 12.4 kg/mol, and PDI = 2.02 (against PS standard).

Poly(3,6-dithien-2-yl-2,5-di(2-octyldodecyl)-pyrrolo[3,4-*c*]-pyrrole-1,4-dione-5′,5″-diyl-*alt*-difluorobenzo 2,1,3-thiadiazol-4,7-diyl] (PDPP-2FBT). Isolated yield of polymer PDPP-2FBT = 100 mg (50%). GPC analysis M_n = 6.6 kg/mol, M_w = 10.9 kg/mol, and PDI = 1.66 (against PS standard).

Typical Procedure for Stille Coupling Polymerization and Polymer Purification. Stannylated DPP (0.20 mmol), dibromo FBT or 2FBT (0.20 mmol), tris(dibenzylidenacetone)dipalladium (0) (1.7 mg, 2.0 μmmol), anhydrous toluene (4 mL) were mixed in a 10 mL of microwave vessel which was purged with argon for 30 min. To this solution, tri(*o*-tolyl)phosphine (1.2 mg, 4.0 μmol) was added and the reaction mixture was heated at 120 °C under vigorous stirring for 6 h using microwave machine. The crude product was poured into a mixture of methanol (300 mL). The resulting solid was filtered off and subjected to sequential Soxhlet extraction with methanol (1 day), acetone (1 day), and hexane (1 day) to remove the low molecular weight fraction of the materials. The residue was extracted with chloroform in order to produce a dark purple product after precipitating again from methanol and drying in vacuo.

Poly(3,6-dithien-2-yl-2,5-di(2-octyldodecyl)-pyrrolo[3,4-*c*]-pyrrole-1,4-dione-5′,5″-diyl-*alt*-fluorobenzo 2,1,3-thiadiazol-4,7-diyl] (PDPP-FBT). Isolated yield of polymer PDPP-FBT = 150 mg (75%). GPC analysis M_n = 24.0 kg/mol, M_w = 48.2 kg/mol, and PDI = 2.01 (against PS standard).

Poly(3,6-dithien-2-yl-2,5-di(2-octyldodecyl)-pyrrolo[3,4-*c*]-pyrrole-1,4-dione-5′,5″-diyl-*alt*-difluorobenzo 2,1,3-thiadiazol-4,7-diyl] (PDPP-2FBT). Isolated yield of polymer PDPP-2FBT = 150 mg (75%). GPC analysis M_n = 25.0 kg/mol, M_w = 58.6 kg/mol, and PDI = 2.34 (against PS standard). Note that the peak assignments and integral values in ^{1}H NMR ($C_2D_2Cl_4$, 600 MHz) spectra of both polymers (**PDDP-FBT** and **PDPP-2FBT**) became very complicated, because of the peak broadening and poor resolution in the aromatic region even at the high temperature (348 K) (see Figure S5 in the Supporting Information).

The thermal properties of **PDPP-FBT** and **PDPP-2FBT** were investigated by thermogravimetric analyses (TGA) and differential scanning calorimetry (DSC). The combination of TGA and DSC data for the both polymers confirmed their good thermal stability without any phase transition processes (see Figure S7 in the Supporting Information).

■ ASSOCIATED CONTENT

Supporting Information

Additional figures (UV, cyclic voltammetry plots, UPS spectroscopy, dipole moment, GIXD data and profiles, TGA, DSC curves, transfer characteristics) and summary of crystallographic parameters, dipole moment, and OFET performance data. This material is available free of charge via the Internet at http://pubs.acs.org.

■ AUTHOR INFORMATION

Corresponding Authors

*E-mail: joonhoh@postech.ac.kr.

*E-mail: yang@unist.ac.kr.

Author Contributions

†J.L. and M.J. contributed equally.

Notes

The authors declare no competing financial interest.

■ ACKNOWLEDGMENTS

This work was supported by the National Research Foundation of Korea (NRF) (2013R1A1A1A05004475, 2014R1A2A2A01007467, 2010-0019408), the Center for Advanced Soft Electronics under the Global Frontier Research Program (2013M3A6A5073175) of the Ministry of Science, ICT and Future Planning, and by the BK21 Plus funded by the Ministry of Education, Korea (10Z20130011057).

■ REFERENCES

(1) Arias, A. C.; MacKenzie, J. D.; McCulloch, I.; Rivnay, J.; Salleo, A. Materials and Applications for Large Area Electronics: Solution-Based Approaches. *Chem. Rev.* **2010**, *110*, 3−24.

(2) Cheng, Y.-J.; Yang, S.-H.; Hsu, C.-S. Synthesis of Conjugated Polymers for Organic Solar Cell Applications. *Chem. Rev.* **2009**, *109*, 5868−5923.

(3) Dhoot, A. S.; Yuen, J. D.; Heeney, M.; McCulloch, I.; Moses, D.; Heeger, A. J. Beyond the Metal-Insulator Transition in Polymer Electrolyte Gated Polymer Field-Effect Transistors. *Proc. Natl. Acad. Sci. U.S.A.* **2006**, *103*, 11834−11837.

(4) Forrest, S. R. The Path to Ubiquitous and Low-Cost Organic Electronic Appliances on Plastic. *Nature* **2004**, *428*, 911−918.

(5) Lee, J.; Han, A.-R.; Kim, J.; Kim, Y.; Oh, J. H.; Yang, C. Solution-Processable Ambipolar Diketopyrrolopyrrole−Selenophene Polymer with Unprecedentedly High Hole and Electron Mobilities. *J. Am. Chem. Soc.* **2012**, *134*, 20713−20721.

(6) Lee, J.; Han, A.-R.; Yu, H.; Shin, T. J.; Yang, C.; Oh, J. H. Boosting the Ambipolar Performance of Solution-Processable Polymer Semiconductors via Hybrid Side-Chain Engineering. *J. Am. Chem. Soc.* **2013**, *135*, 9540−9547.

(7) Liang, Y.; Yu, L. A New Class of Semiconducting Polymers for Bulk Heterojunction Solar Cells with Exceptionally High Performance. *Acc. Chem. Res.* **2010**, *43*, 1227−1236.

(8) McCulloch, I.; Heeney, M.; Bailey, C.; Genevicius, K.; MacDonald, I.; Shkunov, M.; Sparrowe, D.; Tierney, S.; Wagner, R.; Zhang, W.; Chabinyc, M. L.; Kline, R. J.; McGehee, M. D.; Toney, M. F. Liquid-Crystalline Semiconducting Polymers with High Charge-Carrier Mobility. *Nat. Mater.* **2006**, *5*, 328−333.

(9) Murphy, A. R.; Fréchet, J. M. J. Organic Semiconducting Oligomers for Use in Thin Film Transistors. *Chem. Rev.* **2007**, *107*, 1066−1096.

(10) Pan, H.; Li, Y.; Wu, Y.; Liu, P.; Ong, B. S.; Zhu, S.; Xu, G. Low-Temperature, Solution-Processed, High-Mobility Polymer Semiconductors for Thin-Film Transistors. *J. Am. Chem. Soc.* **2007**, *129*, 4112−4113.

(11) Tsao, H. N.; Cho, D. M.; Park, I.; Hansen, M. R.; Mavrinskiy, A.; Yoon, D. Y.; Graf, R.; Pisula, W.; Spiess, H. W.; Müllen, K. Ultrahigh Mobility in Polymer Field-Effect Transistors by Design. *J. Am. Chem. Soc.* **2011**, *133*, 2605−2612.

(12) Yan, H.; Chen, Z.; Zheng, Y.; Newman, C.; Quinn, J. R.; Dotz, F.; Kastler, M.; Facchetti, A. A High-Mobility Electron-Transporting Polymer for Printed Transistors. *Nature* **2009**, *457*, 679−686.

(13) Chen, H.; Guo, Y.; Yu, G.; Zhao, Y.; Zhang, J.; Gao, D.; Liu, H.; Liu, Y. Highly π-Extended Copolymers with Diketopyrrolopyrrole Moieties for High-Performance Field-Effect Transistors. *Adv. Mater.* **2012**, *24*, 4618−4622.

(14) Kang, I.; An, T. K.; Hong, J.-a.; Yun, H.-J.; Kim, R.; Chung, D. S.; Park, C. E.; Kim, Y.-H.; Kwon, S.-K. Effect of Selenophene in a DPP Copolymer Incorporating a Vinyl Group for High-Performance Organic Field-Effect Transistors. *Adv. Mater.* **2013**, *25*, 524−528.

(15) Kang, I.; Yun, H.-J.; Chung, D. S.; Kwon, S.-K.; Kim, Y.-H. Record High Hole Mobility in Polymer Semiconductors via Side-Chain Engineering. *J. Am. Chem. Soc.* **2013**, *135*, 14896−14899.

(16) Kanimozhi, C.; Yaacobi-Gross, N.; Chou, K. W.; Amassian, A.; Anthopoulos, T. D.; Patil, S. Diketopyrrolopyrrole−Diketopyrrolopyrrole-Based Conjugated Copolymer for High-Mobility Organic Field-Effect Transistors. *J. Am. Chem. Soc.* **2012**, *134*, 16532−16535.

(17) Li, J.; Zhao, Y.; Tan, H. S.; Guo, Y.; Di, C.-A.; Yu, G.; Liu, Y.; Lin, M.; Lim, S. H.; Zhou, Y.; Su, H.; Ong, B. S. A Stable Solution-Processed Polymer Semiconductor with Record High-Mobility for Printed Transistors. *Sci. Rep.* **2012**, *2*.

(18) Park, J. H.; Jung, E. H.; Jung, J. W.; Jo, W. H. A Fluorinated Phenylene Unit as a Building Block for High-Performance n-Type Semiconducting Polymer. *Adv. Mater.* **2013**, *25*, 2583−2588.

(19) Lee, J.; Cho, S.; Seo, J. H.; Anant, P.; Jacob, J.; Yang, C. Swapping Field-Effect Transistor Characteristics in Polymeric Diketopyrrolopyrrole Semiconductors: Debut of an Electron Dominant Transporting Polymer. *J. Mater. Chem.* **2012**, *22*, 1504−1510.

(20) Kim, J.; Yun, M. H.; Kim, G.-H.; Lee, J.; Lee, S. M.; Ko, S.-J.; Kim, Y.; Dutta, G. K.; Moon, M.; Park, S. Y.; Kim, D. S.; Kim, J. Y.; Yang, C. Synthesis of PCDTBT-Based Fluorinated Polymers for High Open-Circuit Voltage in Organic Photovoltaics: Towards an Understanding of Relationships between Polymer Energy Levels Engineering and Ideal Morphology Control. *ACS Appl. Mater. Interfaces* **2014**, *6*, 7523−7534.
(21) Albrecht, S.; Janietz, S.; Schindler, W.; Frisch, J.; Kurpiers, J.; Kniepert, J.; Inal, S.; Pingel, P.; Fostiropoulos, K.; Koch, N.; Neher, D. Fluorinated Copolymer Pcpdtbt with Enhanced Open-Circuit Voltage and Reduced Recombination for Highly Efficient Polymer Solar Cells. *J. Am. Chem. Soc.* **2012**, *134*, 14932−14944.
(22) Bronstein, H.; Frost, J. M.; Hadipour, A.; Kim, Y.; Nielsen, C. B.; Ashraf, R. S.; Rand, B. P.; Watkins, S.; McCulloch, I. Effect of Fluorination on the Properties of a Donor−Acceptor Copolymer for Use in Photovoltaic Cells and Transistors. *Chem. Mater.* **2013**, *25*, 277−285.
(23) Dutta, G. K.; Kim, T.; Choi, H.; Lee, J.; Kim, D. S.; Kim, J. Y.; Yang, C. Synthesis of Fluorinated Analogues of a Practical Polymer TQ for Improved Open-Circuit Voltages in Polymer Solar Cells. *Poly. Chem.* **2014**, *5*, 2540−2547.
(24) Schroeder, B. C.; Huang, Z.; Ashraf, R. S.; Smith, J.; D'Angelo, P.; Watkins, S. E.; Anthopoulos, T. D.; Durrant, J. R.; McCulloch, I. Silaindacenodithiophene-Based Low Band Gap Polymers − the Effect of Fluorine Substitution on Device Performances and Film Morphologies. *Adv. Funct. Mater.* **2012**, *22*, 1663−1670.
(25) Stuart, A. C.; Tumbleston, J. R.; Zhou, H.; Li, W.; Liu, S.; Ade, H.; You, W. Fluorine Substituents Reduce Charge Recombination and Drive Structure and Morphology Development in Polymer Solar Cells. *J. Am. Chem. Soc.* **2013**, *135*, 1806−1815.
(26) Zhang, Y.; Chien, S.-C.; Chen, K.-S.; Yip, H.-L.; Sun, Y.; Davies, J. A.; Chen, F.-C.; Jen, A. K.-Y. Increased Open Circuit Voltage in Fluorinated Benzothiadiazole-Based Alternating Conjugated Polymers. *Chem. Commun.* **2011**, *47*, 11026−11028.
(27) Zhou, H.; Yang, L.; Stuart, A. C.; Price, S. C.; Liu, S.; You, W. Development of Fluorinated Benzothiadiazole as a Structural Unit for a Polymer Solar Cell of 7% Efficiency. *Angew. Chem., Int. Ed.* **2011**, *50*, 2995−2998.
(28) Xu, Y.-X.; Chueh, C.-C.; Yip, H.-L.; Ding, F.-Z.; Li, Y.-X.; Li, C.-Z.; Li, X.; Chen, W.-C.; Jen, A. K.-Y. Improved Charge Transport and Absorption Coefficient in Indacenodithieno[3,2-B]Thiophene-Based Ladder-Type Polymer Leading to Highly Efficient Polymer Solar Cells. *Adv. Mater.* **2012**, *24*, 6356−6361.
(29) Dimitrakopoulos, C. D.; Malenfant, P. R. L. Organic Thin Film Transistors for Large Area Electronics. *Adv. Mater.* **2002**, *14*, 99−117.
(30) Facchetti, A.; Mushrush, M.; Yoon, M.-H.; Hutchison, G. R.; Ratner, M. A.; Marks, T. J. Building Blocks for n-Type Molecular and Polymeric Electronics. Perfluoroalkyl-Versus Alkyl-Functionalized Oligothiophenes (Nt; N = 2−6). Systematics of Thin Film Microstructure, Semiconductor Performance, and Modeling of Majority Charge Injection in Field-Effect Transistors. *J. Am. Chem. Soc.* **2004**, *126*, 13859−13874.
(31) Facchetti, A.; Yoon, M.-H.; Stern, C. L.; Katz, H. E.; Marks, T. J. Building Blocks for n-Type Organic Electronics: Regiochemically Modulated Inversion of Majority Carrier Sign in Perfluoroarene-Modified Polythiophene Semiconductors. *Angew. Chem., Int. Ed.* **2003**, *42*, 3900−3903.
(32) Heidenhain, S. B.; Sakamoto, Y.; Suzuki, T.; Miura, A.; Fujikawa, H.; Mori, T.; Tokito, S.; Taga, Y. Perfluorinated Oligo(P-Phenylene)S: Efficient n-Type Semiconductors for Organic Light-Emitting Diodes. *J. Am. Chem. Soc.* **2000**, *122*, 10240−10241.
(33) Jones, B. A.; Facchetti, A.; Wasielewski, M. R.; Marks, T. J. Tuning Orbital Energetics in Arylene Diimide Semiconductors. Materials Design for Ambient Stability of N-Type Charge Transport. *J. Am. Chem. Soc.* **2007**, *129*, 15259−15278.
(34) Sirringhaus, H.; Tessler, N.; Friend, R. H. Integrated Optoelectronic Devices Based on Conjugated Polymers. *Science* **1998**, *280*, 1741−1744.
(35) Bürckstümmer, H.; Weissenstein, A.; Bialas, D.; Würthner, F. Synthesis and Characterization of Optical and Redox Properties of Bithiophene-Functionalized Diketopyrrolopyrrole Chromophores. *J, Org. Chem.* **2011**, *76*, 2426−2432.
(36) Zhao, K.; Khan, H. U.; Li, R.; Su, Y.; Amassian, A. Entanglement of Conjugated Polymer Chains Influences Molecular Self-Assembly and Carrier Transport. *Adv. Funct. Mater.* **2013**, *23*, 6024−6035.
(37) Barder, T. E.; Walker, S. D.; Martinelli, J. R.; Buchwald, S. L. Catalysts for Suzuki−Miyaura Coupling Processes: Scope and Studies of the Effect of Ligand Structure. *J. Am. Chem. Soc.* **2005**, *127*, 4685−4696.
(38) Billingsley, K.; Buchwald, S. L. Highly Efficient Monophosphine-Based Catalyst for the Palladium-Catalyzed Suzuki−Miyaura Reaction of Heteroaryl Halides and Heteroaryl Boronic Acids and Esters. *J. Am. Chem. Soc.* **2007**, *129*, 3358−3366.
(39) Kinzel, T.; Zhang, Y.; Buchwald, S. L. A New Palladium Precatalyst Allows for the Fast Suzuki−Miyaura Coupling Reactions of Unstable Polyfluorophenyl and 2-Heteroaryl Boronic Acids. *J. Am. Chem. Soc.* **2010**, *132*, 14073−14075.
(40) Martin, R.; Buchwald, S. L. Palladium-Catalyzed Suzuki−Miyaura Cross-Coupling Reactions Employing Dialkylbiaryl Phosphine Ligands. *Acc. Chem. Res.* **2008**, *41*, 1461−1473.
(41) Ahmed, M.; Pisula, W.; Mhaisalkar, S. Synthesis and Characterization of New Thieno[3,2-B]Thiophene Derivatives. *Molecules* **2012**, *17*, 12163−12171.
(42) Stille, J. K. The Palladium-Catalyzed Cross-Coupling Reactions of Organotin Reagents with Organic Electrophiles [New Synthetic Methods (58)]. *Angew. Chem., Int. Ed.* **1986**, *25*, 508−524.
(43) Cho, S.; Lee, J.; Tong, M.; Seo, J. H.; Yang, C. Poly(Diketopyrrolopyrrole-Benzothiadiazole) with Ambipolarity Approaching 100% Equivalency. *Adv. Funct. Mater.* **2011**, *21*, 1910−1916.
(44) Wallquist, O.; Lenz, R. 20 Years of DPP Pigments-Future Perspectives. *Macromol. Symp.* **2002**, *187*, 617−630.
(45) Sonar, P.; Singh, S. P.; Li, Y.; Soh, M. S.; Dodabalapur, A. A Low-Bandgap Diketopyrrolopyrrole-Benzothiadiazole-Based Copolymer for High-Mobility Ambipolar Organic Thin-Film Transistors. *Adv. Mater.* **2010**, *22*, 5409−5413.
(46) Lee, W. Y.; Giri, G.; Diao, Y.; Tassone, C. J.; Matthews, J. R.; Sorensen, M. L.; Mannsfeld, S. C. B.; Chen, W. C.; Fong, H. H.; Tok, J. B. H.; Toney, M. F.; He, M. Q.; Bao, Z. A. Effect of Non-Chlorinated Mixed Solvents on Charge Transport and Morphology of Solution-Processed Polymer Field-Effect Transistors. *Adv. Funct. Mater.* **2014**, *24*, 3524−3534.
(47) Chang, J.-F.; Sun, B.; Breiby, D. W.; Nielsen, M. M.; Sölling, T. I.; Giles, M.; McCulloch, I.; Sirringhaus, H. Enhanced Mobility of Poly(3-Hexylthiophene) Transistors by Spin-Coating from High-Boiling-Point Solvents. *Chem. Mater.* **2004**, *16*, 4772−4776.
(48) Lin, H.-W.; Lee, W.-Y.; Chen, W.-C. Selenophene-DPP Donor-Acceptor Conjugated Polymer for High Performance Ambipolar Field Effect Transistor and Nonvolatile Memory Applications. *J. Mater. Chem.* **2012**, *22*, 2120−2128.
(49) Liu, C.; Li, Y.; Minari, T.; Takimiya, K.; Tsukagoshi, K. Forming Semiconductor/Dielectric Double Layers by One-Step Spin-Coating for Enhancing the Performance of Organic Field-Effect Transistors. *Org. Electron.* **2012**, *13*, 1146−1151.
(50) Yum, S.; An, T. K.; Wang, X.; Lee, W.; Uddin, M. A.; Kim, Y. J.; Nguyen, T. L.; Xu, S.; Hwang, S.; Park, C. E.; Woo, H. Y. Benzotriazole-Containing Planar Conjugated Polymers with Non-covalent Conformational Locks for Thermally Stable and Efficient Polymer Field-Effect Transistors. *Chem. Mater.* **2014**, *26*, 2147−2154.
(51) Schmidt, R.; Ling, M. M.; Oh, J. H.; Winkler, M.; Könemann, M.; Bao, Z.; Würthner, F. Core-Fluorinated Perylene Bisimide Dyes: Air Stable N-Channel Organic Semiconductors for Thin Film Transistors with Exceptionally High On-to-Off Current Ratios. *Adv. Mater.* **2007**, *19*, 3692−3695.
(52) Kim, K.-H.; Yu, H.; Kang, H.; Kang, D. J.; Cho, C.-H.; Cho, H.-H.; Oh, J. H.; Kim, B. J. Influence of Intermolecular Interactions of Electron Donating Small Molecules on Their Molecular Packing and

Performance in Organic Electronic Devices. *J. Mater. Chem. A* **2013**, *1*, 14538−14547.
(53) Oh, J. H.; Sun, Y.-S.; Schmidt, R.; Toney, M. F.; Nordlund, D.; Könemann, M.; Würthner, F.; Bao, Z. Interplay between Energetic and Kinetic Factors on the Ambient Stability of N-Channel Organic Transistors Based on Perylene Diimide Derivatives. *Chem. Mater.* **2009**, *21*, 5508−5518.
(54) Chen, Z.; Lee, M. J.; Shahid Ashraf, R.; Gu, Y.; Albert-Seifried, S.; Meedom Nielsen, M.; Schroeder, B.; Anthopoulos, T. D.; Heeney, M.; McCulloch, I.; Sirringhaus, H. High-Performance Ambipolar Diketopyrrolopyrrole-Thieno[3,2-B]Thiophene Copolymer Field-Effect Transistors with Balanced Hole and Electron Mobilities. *Adv. Mater.* **2012**, *24*, 647−652.
(55) Graz, I. M.; Lacour, S. P. Complementary Organic Thin Film Transistor Circuits Fabricated Directly on Silicone Substrates. *Org. Electron.* **2010**, *11*, 1815−1820.
(56) Hu, X.; Zuo, L.; Fu, W.; Larsen-Olsen, T. T.; Helgesen, M.; Bundgaard, E.; Hagemann, O.; Shi, M.; Krebs, F. C.; Chen, H. Incorporation of Ester Groups into Low Band-Gap Diketopyrrolopyrrole Containing Polymers for Solar Cell Applications. *J. Mater. Chem.* **2012**, *22*, 15710−15716.